A modeling approach to determine the importance of dynamic regulation of plant hydraulic conductivities on the water uptake dynamics in the soil-plant-atmosphere system

Guillaume Lobet[a,b], Loïc Pagès[c], Xavier Draye[b,*]

[a] *Current address: PhytoSYSTEMS, Université de Liège, Belgium*
[b] *Earth and Life Institute, Université catholique de Louvain, Belgium*
[c] *INRA, Avignon, France*

Abstract

We present here a new model, PlaNet-Maize, with the purpose of investigating the effect of environmental and endogenous factors on the growth and water relations of the maize plant. This functional-structural plant model (FSPM) encompasses the entire soil-plant-atmosphere continuum with a sub-organ resolution. The model simulates the growth and development of an individual maize plant and the flux of water through the plant structure, from the rhizosphere to the leaf boundary layer. Leaf stomatal conductance and root radial and axial conductivities are considered as functions of local water potential. Finally, a simple carbon allocation rule is included in the model to allow the feedback effect of water deficit on plant growth. The model was successfully used to reproduce experimental plant hydraulic behavior in

*Corresponding author
Email addresses: guillaume.lobet@ulg.ac.be (Guillaume Lobet), loic.pages@inra.avignon.fr (Loïc Pagès), xavier.draye@uclouvain.be (Xavier Draye)

response to water deficit. The quantitative contribution of leaf conductance and root conductivities were assessed individually and in combination.

Our results highlight the importance of regulating hydraulic properties in FSPM as these can strongly modify the water uptake dynamics and lead to emerging water uptake behaviors. The modeling results also indicate that plant hydraulic properties can theoretically be tailored to improve plant water use in challenging environments.

Keywords:
maize, water uptake dynamics, functional-structural plant model

---

1. Introduction

The flow of water in the soil-plant-atmosphere continuum is a passive process driven by water potential differences and enabled by the continuity of the liquid phase of water between the soil and the leaf mesophyl (Steudle, 2001). For a given driving force, the flow of water in the plant is set primarily, though not exclusively, by the radial conductance of the root system, the axial conductivity of the xylem and the leaf conductance.

The leaf conductance, which is largely determined by the density and aperture of the stomata, sets the maximum amount of water that can be transpired under a given environmental demand. Due to the obvious and major role of stomata, the mechanisms underlying their regulation have received much attention from the scientific community, leading to numerous

experimental and modeling approaches (reviewed by Damour et al. (2010)).

The root radial conductance is a complex property reflecting the composite nature of water movement from the root surface to the xylem. It both depends on irreversible processes like the deposition of hydrophobic barriers in the endodermis and exodermis (Enstone et al., 2003), and on time-varying features like the activity of water channels (Maurel et al., 2008; Javot and Maurel, 2002). The crossing of root tissues is generally considered as an important limiting step in the water uptake process (Steudle and Peterson, 1998).

The axial conductivity of the xylem vessels is also a complex property which combines the structural features of the xylem, the dynamics of cavitation events occurring when the tension in the xylem is too large (Sperry et al., 1998) and the extent of embolized vessels refilling that occurs when the tension vanishes but possibly also under tension (McCully et al., 1998; Zwieniecki and Holbrook, 2009; Holbrook and Zwieniecki, 1999).

While the leaf conductance sets the amount of water extracted by the plant, the distribution of root axial conductivities and radial conductances throughout the root system (the *hydraulic architecture*) determines the sites of water uptake in the soil. This role of root hydraulic properties has often been considered as minor in comparison with root length density, but this should be reconsidered in view of recent data (Draye et al., 2010). Therefore, considering leaf, root and environmental factors simultaneously may be an important contribution if we aim to tailor plants with improved resistance to water deficit.

For many years, scientists have developed computer models to simulate how biological processes, described individually or at an organ scale, integrate and scale up in the soil-plant-atmosphere system. On the root side, models evolved from architectural models reproducing the root system shape and growth (Diggle, 1988; Pagès et al., 1989; Lynch et al., 1997) to functional-structural models simulating physical, chemical or physiological processes such as nutrient acquisition (Ge et al., 2000), carbon allocation (Bidel et al., 2000) or water uptake (Somma et al., 1998; Javaux et al., 2008). A similar trend was observed for shoot models (Fournier and Andrieu, 1998). While some models address simultaneously the root and shoot systems (Drouet and Pagès, 2003; Janott et al., 2011), the vast majority focus on either part of the plant and use simplified descriptions of the other. As of today, we are not aware of any model that simulates the water dynamics of a complete plant with a detailed description of each organ.

This situation led us to develop the PlaNet-Maize model, which simulates at a sub-organ resolution the growth and architecture, the water flows and the main hydraulic regulations of a whole maize plant. The model uses simplified rules for the production and allocation of assimilates to the different organs.

2. Model description

2.1. General principles

PlaNet-Maize adheres to the principles of the metal-model PlaNet (Plant as a Network), developed by Loïc Pagès, that defines a building schema for the creation of various whole plant models. In PlaNet, the plant structure is viewed as a network of articles interconnected in a tree-like structure and localized in space. Articles are typically organs, but can be defined as smaller or larger entities. They have three fundamental behaviors: (1) they can grow and create new articles (morpho-generator), (2) they have their own metabolic activity (bio-reactor) and (3) they can transport substances from and to neighboring articles and environment (carrier). As articles are localized in space and in the network topology, these behaviors can be dependent on local environment information as well as on network-derived information.

Two types of articles are typically considered in PlaNet. The first are the segments, which make up the structure of the plant. The second are the meristems, which generate new segments and / or meristems and ensure growth and branching. These two types of articles can be sub-divided based on their botanical nature: stem, leaf or root. These six types of articles are sufficient to simulate the growth and development of a whole plant during the vegetative stage (fig. 1).

The PlaNet-Maize model uses PlaNet rules to simulate the growth and structure of a maize plant and includes modules specific to water movement and hydraulic regulatory processes. PlaNet-Maize was developed in Java and

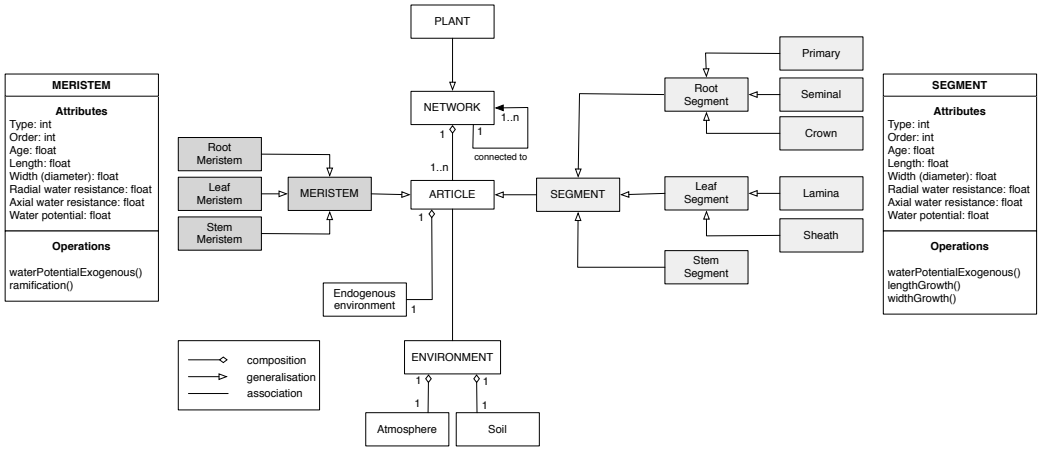

Figure 1: PlaNet-Maize UML scheme. Light grey boxes represent the segments classes. Dark grey boxes represent the meristem classes.

is integrated in the modeling platform CrossTalk (Draye and Pagès, 2006) that enables the coupling with environment models, the 3D visualization and the *in situ* interactive modification of the plant during a simulation (e.g. pruning). The CrossTalk platform allows users to easily modify a simulation parameters such as the initial environmental condition or the simulation time-step (in hours).

2.2. Architecture module

2.2.1. Root system

The root system of PlaNet-Maize comprises four types of roots: the primary root (first embryonic root), the seminal roots (embryonic roots initiated from the scutelar node), the crown roots (shoot-born roots) and the first and second order lateral roots (Hochholdinder et al., 2004). Its implementa-

tion was inspired from previous root architecture models (Pagès et al., 2004; Drouet and Pagès, 2003) with the distinction that root axes in PlaNet-Maize originate from different types of organs (fig. 2.B). The primary and seminal roots arise from the seed while crown root meristems are initiated by the stem meristem. It follows that there is no single connection between the root system and the shoot and that preferential water flow may occur between crown roots and the leaf initiated at the same node. Root elongation rate was computed as a function of the root meristem diameter (Drouet and Pagès, 2003; Mollier and PEllerin, 1999).

2.2.2. Shoot system

The shoot architectural module of PlaNet-Maize was largely inspired from the model GRAAL where leaf and stem growth and development are determined by morphogenetic processes and are functions of thermal time (Drouet and Pagès, 2003). Similarly as for the roots, leaves are made of successive segment articles. Every article is labeled as part of the sheath or the lamina. The leaf meristem is located at the junction between the sheath and the lamina (fig. 2.B).

2.3. Carbon module

A carbon module was implemented in PlaNet-Maize to allow various feedbacks between plant growth and water dynamics. For the sake of simplicity, the carbon module was not implemented at article but at plant level. The module was divided into three processes: production, demand and allocation of assimilates.

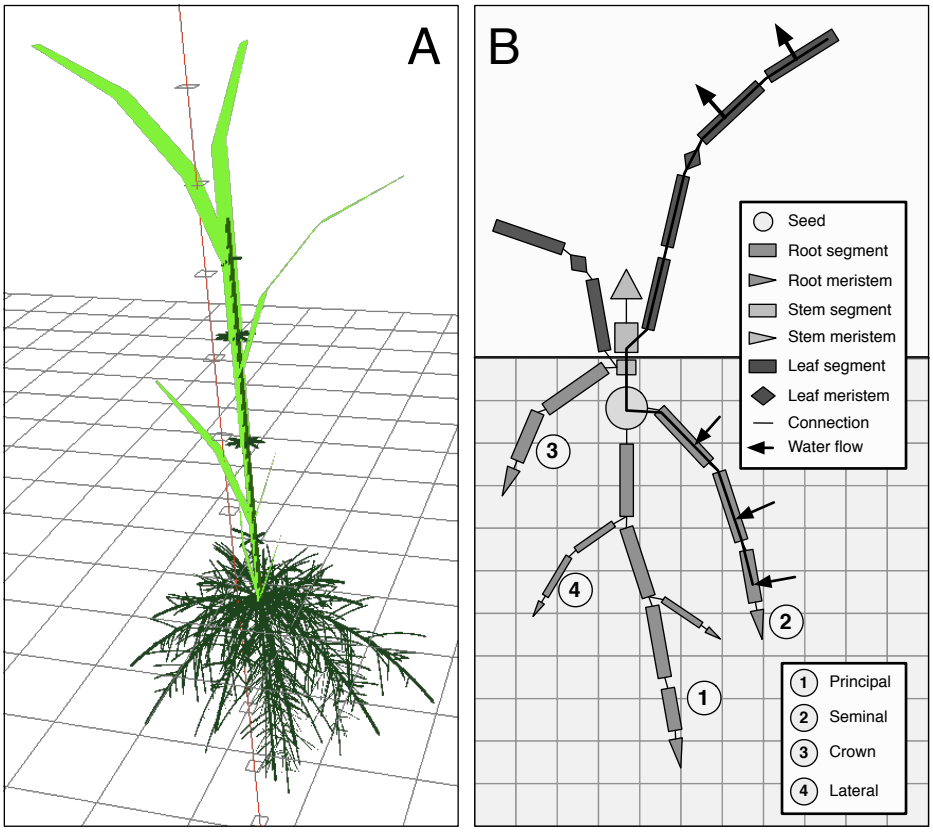

Figure 2: PlaNet-Maize representations. A. PlaNet-Maize visual output in CrossTalk. B. Schematic representation of the PlaNet-Maize structure.

2.3.1. Production

During the first steps of the simulation, the seed acts as a carbon source and its supply is computed at each time step according to the seed dry weight and a seed supply rate factor. When leaves start transpiring, the amount of carbon produced at each time step (C_{av}) is defined by the total amount of water transpired by the plant as in the model presented by Somma et al. (1998) and considering instantaneous water use efficiency values between 3.5 and 9.5 $\mathrm{mg}_{CO_2}/\mathrm{g}_{H_2O}$ (Allen et al., 2011). Finally, at each time step, exceeding carbon (see below) is stored and can be further released as a function of the total amount of C available at the plant level and a reserve supply rate (Drouet and Pagès, 2003).

2.3.2. Demand

Carbon demand is divided into maintenance and growth demands. The maintenance demand is computed for every plant article such as:

$$C_m = mMQ10^{(T-T_{ref})/10}\Delta t \tag{1}$$

where C_m is the carbon maintenance demand [g_{CO_2}], M is the organ dry mass [g], m the specific maintenance cost [$\mathrm{g}_{C0_2}.\mathrm{g}^{-1}\mathrm{DM}$], $Q10$ is a temperature coefficient [-], T is the environmental temperature [^{o}C], T_{ref} is the temperature above which maintenance cost is more than proportional to the organ dry mass [^{o}C] and Δt is the length of the time step [h] (Drouet and Pagès, 2003).

Similarly, the growth demand is defined for every article following the equation:

$$C_g = \frac{G_p}{g}\Delta t \tag{2}$$

where C_g is the carbon growth demand [g_{CO_2}/h], G_p is the potential growth in dry mass [g_{CO_2}], g is a growth conversion coefficient [-] and Δt is the length of the time step [h] (Drouet and Pagès, 2003). The dry mass of every article is a function of its volume and density, depending on the article age (Drouet and Pagès, 2003, 2007).

2.3.3. Allocation

The allocation of the available carbon (C_{av}) between all plant articles follows precise priority rules. C_{av} is used in priority to meet the whole plant maintenance demand, considered as an obligatory cost (Drouet and Pagès, 2003; Postma and Lynch, 2011). The remaining C:

$$C_{avg} = C_{av} - C_m, \tag{3}$$

is divided between the root and the shoot according to a root-to-shoot C allocation ratio (0.6, Somma et al. (1998)). In the shoot, priority is given to the leaf growth over the stem, while in the roots, priority is defined based on the potential growth rate of each root (*sink term*). Once this allocation is performed, a growth satisfaction coefficient is computed for every article ($G_p.C_{avg}^{-1}$, between 0 and 1). This coefficient will be used (1) to define the actual growth of the different articles and (2) to define the initial diameter of newly created root meristems. As in the GRAAL model, if this diameter falls under a critical minimum value (0.14 cm, Drouet and Pagès (2003)), the meristem is not initiated.

2.4. Water fluxes module

2.4.1. General principle

The network of articles intervening in the uptake and transport of water in the plant can be conveniently analyzed using the analogy with an electric circuit (Landsberg and Fowkes, 1978). In particular, radial water fluxes can be described using the equation:

$$J_r(z) = L_r[\psi_e(z) - \psi_x(z)]S \tag{4}$$

where $J_r(z)$ is the radial flux through root tissues or stomata [$m^3.s^{-1}$], $\psi_x(z)$ and $\psi_e(z)$ are respectively the water potential of the article (viz. xylem) and of the environment [MPa], L_r is the article radial conductivity [$m.s^{-1}.MPa^{-1}$] and S is the article surface [m^2]. Similarly, the axial water flux can be described as follow:

$$J_h(z) = -K_h \frac{\Delta\psi_x(z)}{\Delta z} \tag{5}$$

where $J_h(z)$ is the axial flux between two articles [$m^3.s^{-1}$], $-K_h$ is the xylem conductance [$m^4.s^{-1}.MPa^{-1}$], $\Delta\psi_x(z)$ is the water potential difference between the articles and Δz is the distance between these articles [m]. Finally, the Kirchhoff law, which states that *in* fluxes must equal *out* fluxes, is applied to every article:

$$\sum^{k} I_{kin} = \sum^{k} I_{kout} \tag{6}$$

The combination of these three equations has been successfully used to simulate water transfers in the soil-plant system in different models (Doussan et al., 2006; Javaux et al., 2008). In these models, at each time step, the equations are specified for every root segment and are assembled as a system of linear equations that is solvable for all articles that comprise the root system. In PlaNet-Maize, we generalized this formulation in order to apply it to the whole plant level (roots, stem and leaves).

2.4.2. Soil water depletion

The soil in PlaNet-Maize is implemented as a 3D grid of voxels with a mesh size of typically 1 cm^3. Soil water depletion is simulated by removing the uptake of every root article from its enclosing voxel. The relationship between the soil water content and the soil water potential (θ-h curve) is defined using a Mualen-van Genuchten equation (van Genuchten, 1980) and based on experimental measurement (data not shown).

It has to be noted that the current implementation of water fluxes in the soil 3D domain does not follow Richard's equation (unlike traditional soil models like HYDRUS). In PlaNet-Maize, horizontal redistribution of water in the bulk soil is obtained by the application of a mean smoothing operator on every soil element and its 4 horizontal neighbors. This operator may be modified to simulate different soil properties. Despite the fact that this method lacks physical basis, it has the advantage to mimic basic soil water movement at a minimum computational cost.

2.4.3. Hydraulic parameters

To the exception of the stomatal conductance, most of the conductances used in the water flux module remain poorly estimated experimentally. In addition, some of these conductances are expressed in different units. In particular, the root radial conductivity is expressed in [m.s^{-1}.MPa^{-1}] while the leaf radial conductivity (g_s) is usually expressed in [m^3.m^{-2}.s^{-1}]), which lead us to make some approximation in the model.

Root. The root hydraulic properties described by Doussan et al. (1998) were used in this study. These properties (axial and radial) are functions of the root segment age and type (axis or lateral). These values have been used successfully in previous models (Doussan et al., 2006; Javaux et al., 2008).

Stem. The stem radial conductivity was set to zero, assuming that the stem is not permeable to water. Its axial conductivity was calculated according to the Hagen-Poiseuille law,

$$K = \frac{\Pi r^4}{8\eta} \tag{7}$$

where K is the axial conductivity, r the radius of the xylem pipes and η the water dynamic viscosity (= 1.002 mPa.s). Xylem radius was estimated to be 1.7% of the stem radius (Li et al., 2009). In our case, for the sake of simplicity, xylem vessels were considered as a single pipe.

Leaves. As few quantitative data about the axial conductivity of the leaf were found in the literature, we set it to a tenth of the stem axial conductivity (Wei et al., 1999). As mentioned above, leaf radial conductivity values are generally based on the difference in relative humidity between the stomatal

cavity and the atmosphere and do not fit the water flux resolution in PlaNet-Maize that are based on on water potential differences. Therefore, we used the flux equation

$$L_r = \frac{\Delta\psi S}{J_{out}} \tag{8}$$

where $\Delta\psi$ is the water potential difference between the atmosphere and the leaf [MPa], S is the leaf area [cm^2] and J_{out} the radial water flux [$m.s^{-1}$], with experimental data on water potential and flux (not shown), and could estimate the maximal leaf stomatal conductance to $3x10^9 m.s^{-1}.MPa^{-1}$.

2.4.4. Hydraulic regulation of the plant

In order to investigate the contribution of varying hydraulic properties to the regulation of the water status of the plant, we introduced modifier functions that reduce the radial conductance of roots, the axial conductivity of the xylem (roots, stem and leaf) and the leaf radial conductance. These modifiers were calculated locally for each article as a function of their (xylem) water potential.

Leaf conductance (g_s). As stomata, which ranges from fully open to completely closed, ultimately define the transpiration demand, their regulation is therefore seen as the master control site in the transpiration flow. In PlaNet-Maize, stomatal closure is influenced by exogenous (light, temperature and vapor pressure deficit) and endogenous (leaf water potential) factors. Diurnal variations in the leaf stomatal conductivity due to exogenous factors were implemented following the Jarvis equation (Jarvis, 1976):

$$g_s = g_{smax} * F_1(PAR) * F_2(T_a) * F_3(VPD) \quad (9)$$

where g_s is the leaf stomatal conductance [mm.s^{-1}] and g_{smax} is the maximum stomatal conductance of individual leaves under optimal conditions [mm.s^{-1}]. $F_1(PAR)$, $F_2(T_a)$ and $F_3(VPD)$ are environmental stress functions, with $0 \leq F_i(X) \leq 1$. For the sake of simplicity, light interception was not computed as a function of leaf positioning and mutual shading.

The influence of the leaf water potential on the leaf radial conductivity (fig. 3.A) was implemented in PlaNet-Maize using a Weibull function (Janott et al., 2011; Bohrer et al., 2005) following data from Cochard (2002):

$$f(\psi) = 1 - e^{-(-\frac{\psi}{b})^c} \quad (10)$$

where b and c are curve parameters and ψ is the article water potential.

Root radial conductivity (K_r). The dynamic regulation of the root radial conductivity is mainly performed through the regulation of aquaporin activity (Maurel et al., 2008; Javot and Maurel, 2002), although quantitative data linking aquaporin activity with the root radial conductivity are generally not available. Aquaporin activity is down regulated during water deficit, yet it is not clear to what extent aquaporin activity influences K_r (Bramley et al., 2009). Therefore, the regulation of root radial conductivity was implemented in PlaNet-Maize following a logistic function bounded between 1 and 0.4, considering that aquaporin regulation cannot reduce the root radial conductivity to zero (fig. 3.A).

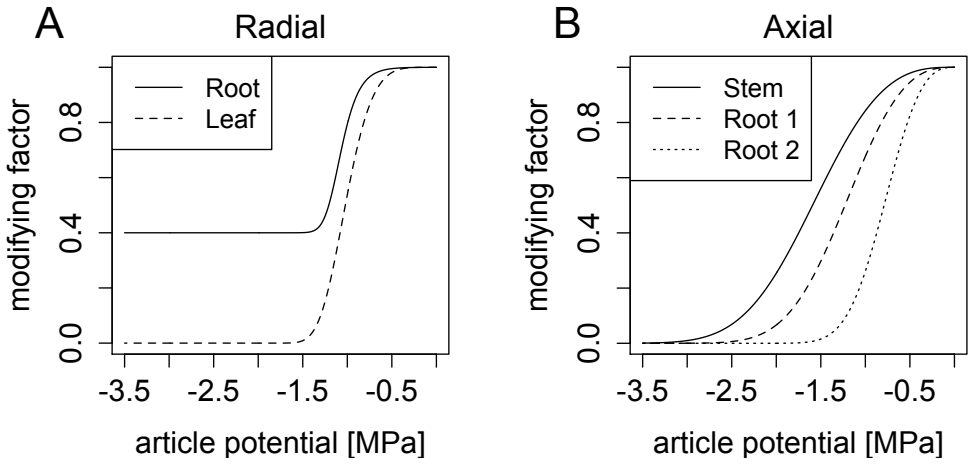

Figure 3: PlaNet-Maize conductivity modifiers. A. Modifiers for root/leaf radial conductivities. B. Modifiers for the axial conductance. PR = first order root. LR = lateral root.

Axial conductance (K_x). Changes of axial conductance occur primarily under the influence of xylem cavitation and embolism repair (Peirce, 1936). The relationship between the tension in the xylem and the decrease in axial conductance is commonly described using Weibull functions (Sperry et al., 1988; Tyree and Sperry, 1989) (see eq. 10). In PlaNet-Maize , the Weibull function was implemented in every article according to data from Li et al. (2009) and considering different curves for the different plant organs (stem > first order roots > second order roots, fig. 3.B, Hacke et al. (2000a)).

3. Method

3.1. Conditions for simulations

The aim of the simulations presented here was to assess the significance of the intimate processes by which the maize plant regulates its water uptake

behavior (hence its water status) by modifying architectural and/or hydraulic traits. Four sets of simulations were performed. The first set (I, tab. 1) highlights the effect of the root-to-shoot surface ratio (RSSR) by changing the number of seminal roots for given hydraulic parameters and transpiration demand. The second set of simulations (II, tab. 1) focuses on the effect of conductivity modifiers. The third set (IIIa-d, tab. 1) simulates the influence of management practices (well-watered, water-stressed, deficit irrigation and partial root-zone drying). Finally, the last set (IVa-f, tab. 1) was used to analyze the sensitivity of the water flow regulation mechanisms.

In all simulations, the soil and atmosphere initial water potential were respectively set to -0.01 and -95 MPa. Environmental conditions (temperature, light and VPD) were set according to a summer day in a greenhouse in Louvain-la-Neuve (Belgium, $+50^o$ 39' 59.91", $+4^o$ 37' 10.56"). A sandy soil with a low water retention capacity was considered in order to observe rapid water shortage for the plant. The simulation time step was 1h for the plant development and 10 minutes for the water fluxes. Data were exported every 12 hours, from the 50^{th} to the 350^{th} hour of the simulations.

3.2. Effect of root system size and hydraulic regulations

Water uptake by plants can be considered in economical terms, the shoot and the root defining respectively a potential demand and a supply capacity. In the plant-soil system, the evaporative demand is mainly defined by the leaf area, the stomatal conductance (g_s) and the VPD. On the other hand, the supply capacity is set by the root system architecture, its hydraulic properties and the local soil water potential (Draye et al., 2010; Lobet et al., 2013). When the demand exceeds the supply capacity, the system is put under strain

Table 1: Conditions for simulations. PRD = partial root zone drying. RW = Rewatering. # of SR = number of seminal roots

Simulation	# of SR	regulation	carbon	water depletion
I	0-6	none	no	no
II	0-6	all	no	no
IIIa	4	all	yes	no
IIIb	4	all	yes	yes
IIIc	4	all	yes	PRD
IIId	4	all	yes	RW
IVa	4	enhanced g_s	yes	yes
IVb	4	inhibited g_s	yes	yes
IVc	4	enhanced K_r	yes	yes
IVd	4	inhibited K_r	yes	yes
IVe	4	enhanced K_x	yes	yes
IVf	4	inhibited K_x	yes	yes

until the demand decreases or the supply increases.

In order to test the effect of the root-to-shoot surface ratio (RSSR) on the hydraulic status of the plant, simulations with different initial numbers of seminal roots (between 0 and 6) and with the same root growth rate and shoot system development were performed. The carbon module was disabled to avoid feedbacks between transpiration, growth and C allocation (growth rates were set to their potential values).

In the first set of simulations, the hydraulic regulation and soil water depletion were disabled to isolate the effect of the root system size (tab. 1.I). These were enabled in the second set of simulations, through the use of modifier functions (tab. 1.II).

3.3. Effect of irrigation practices

Four watering scenarios were simulated in order to compare the response of plants to different water management practices (tab. 1.III): well-watered (WW), water deficit (WD), partial root zone drying (PRD) and re-watering (RW). In the WW treatment, the soil water potential was maintained at a constant value (field capacity) during the whole simulation while in the WD treatment, the absorbed water was depleted from the corresponding soil voxels and a basic horizontal redistribution of water in the soil was enabled. In the PRD treatment, the soil domain was split vertically in two compartments simulated respectively as WW and WD. Finally, in the RW simulation, the soil was treated as in the WD treatment, except that re-watering events were

simulated every 100 hours by resetting the initial soil water potential in all voxels (fig. 7.A). All treatments were applied from the beginning of the simulations.

3.4. Effect of regulation sensibility

Finally, sensitivity analysis was performed to assess the effect of the regulation of g_s, K_r and K_x implemented through the use of modifiers (tab. 1.IV). For each conductance, the modifier function was shifted towards lower and higher water potential values, leading, respectively to delayed and faster responses to changes in water potential (fig. 4). This analysis revealed contrasting differences between the relative effects of the three regulation processes.

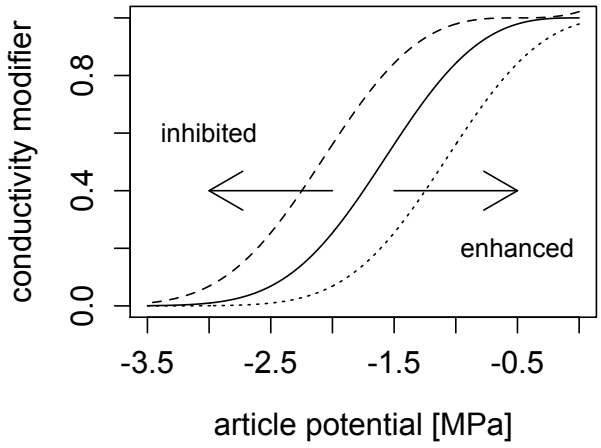

Figure 4: Regulation sensibility. Plain line represents the control regulation curve. Dashed line represent the delayed response. Dotted line represent the faster response.

4. Results and discussions

4.1. Model comparison with experimental data

The architectural and water flux modules were compared against experimental data independent of the one used to calibrate the model (Girardin, 2000; Hu et al., 2011; Postma and Lynch, 2011; Mollier and PEllerin, 1999). PlaNet-Maize was able to reproduce realistic kinetics of root and shoot growth and water fluxes, integrated at the plant level (fig. 5). Since the aim of the model was not to reproduce a specific genotype X environment combination, but rather explore the dynamic of the system, we estimated such similarity between simulated and experimental data was sufficient to validate the model.

4.2. Root system size and hydraulic regulations

Figure 6.A summarizes the relationship between RSSR and the plant water potential (computed at the collar level). Considering a permanent wilting point at -1.5 MPa, the simulations suggest that a minimum RSSR value of 2.0 is needed for a theoretical plant that would not regulate its root, leaf and axial conductances. Allowing the plant to regulate these hydraulic properties widens the range of viable RSSR values (fig. 6.B).

These simulation results show that a shoot:root allometry is beneficial for the maintenance of water potential values above the permanent wilting point (-1.5 MPa). They also indicate that the regulation of hydraulic properties contributes to stabilize the plant water potential but does not completely

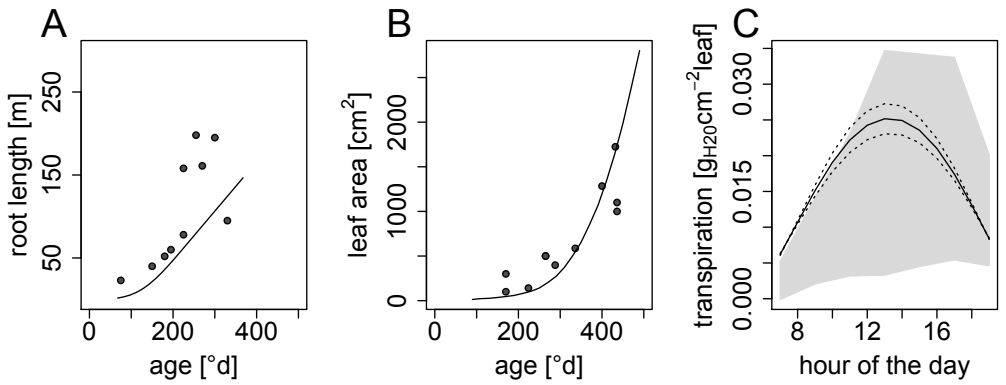

Figure 5: Comparison between experimental and simulated data. A. Comparison between experimental (circles, data from Hu et al. (2011); Mollier and PEllerin (1999)) and simulated (line) root length values. B. Comparison between experimental (circles, data from Girardin (2000); Postma and Lynch (2011)) and simulated (line) shoot area values. C. Comparison between experimental (grey area) obtained in greenhouse experiment (same environmental condition as for the simulations) and simulated (lines) transpiration values. Plain line represents the mean simulated transpiration value while the dashed lines represent the standard deviation range due to day to day variations .

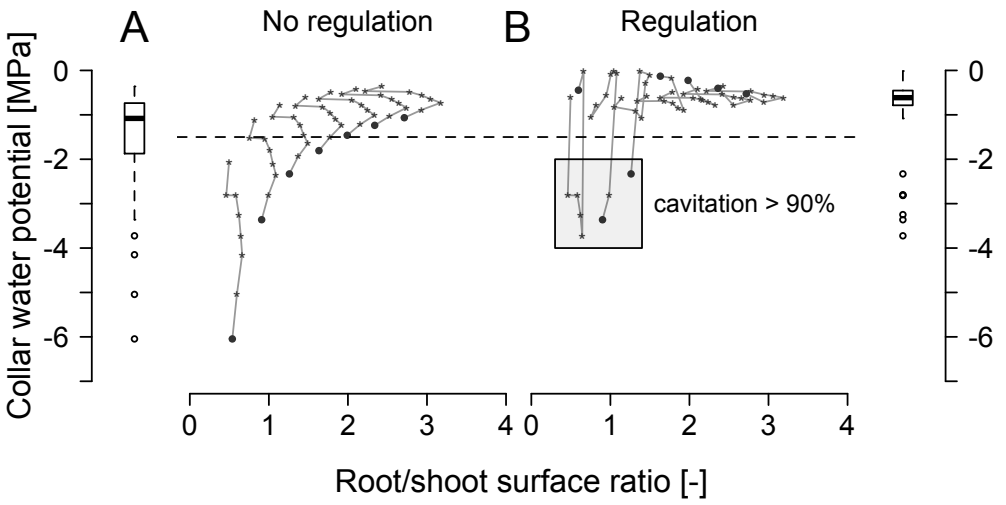

Figure 6: Relationship between the Root-to-shoot surface ratio and the collar water potential. A. Without hydraulic regulation. B. With hydraulic regulation. Dashed lines represent the permanent wilting point (-1.5 MPa). Each point represent the collar water potential at noon at different days, with plain circles representing the last day of simulation. Lines connect points from the same plant to highlight the dynamic of the system. In B, the grey box indicate the points were cavitation in the plant exceed 90% of the total system. Distribution of water potentials are highlighted by the boxplots on either side of the graph.

overcome the effect of structural allometry. As such, the simulations reproduce many experimental results that showed that an undersized root system leads to greater tension in the xylem, leading to important cavitation events (fig. 6.B, grey box, Hacke et al. (2000b); Sperry et al. (1998). The simulations also suggest that the range of viable root-to-shoot ratios is rather large and influenced by the hydraulic regulation strategy used by plants.

4.3. Hydraulic signals alone are not sufficient to reproduce the effects of different irrigation practices

Compared to WW, all treatments led to a clear reduction of the soil water potential. The PRD was able to maintain the soil water potential at a lower but stable value until 250 hours, thereby avoiding the abrupt transitions that occur in the RW treatment (fig. 7.A).

Not surprisingly, reducing the water availability for the plant had a direct effect on the transpiration (fig. 7.B). Consistently with the soil water potential evolution, WD plants presented the lowest transpiration, while the PRD and RW scenario generated intermediate transpiration. The reduction of transpiration, in turn, led to a reduction of plant growth, although relatively small (fig. 7.C).

Throughout the simulation, the leaf water potential displayed a regular decline in all treatments, which should be attributed to a decrease in the RSSR (fig. 7.D). Interestingly, until 250 hours, the leaf water potential difference between the different treatments and WW were similar to the soil water potential difference.

Figure 8 describes the influence of the irrigation technique on the root water status. WD plants have smaller root systems, lower root water potential and conductivities and also a reduced uptake compared to the WW plant. It is unclear wether the latter results from the smaller uptake capacity (root surface) and/or the smaller demand (leaf size and leaf conductance). As for the previous results, the PRD and RW scenarios exhibit intermediate values.

One should notice that the water uptake profiles did not strictly correspond to the root surface profiles, particularly for the WD plant. The phenomenon, known as the compensation mechanism (Draye et al., 2010; Couvreur et al., 2012) arises when regions of the root system are surrounded by a soil layer that has a lower conductivity than the soil in the vicinity of the rest of the root system, or when the integrated conductance between roots and the collar differ among roots. When this occurs, the water uptake by roots with low soil/root conductances will be lowered and compensated by a larger water uptake by the other roots. This occurs typically in the WD, in the non-irrigated part of the PRD and in the RW treatments, where the lower root water potential increases water uptake with depth. In other words, uptake sites are not only defined by the root placement in the soil. They depend on the integration of the root system architecture, the root hydraulic properties and the water availability in the surrounding soil. (Draye et al., 2010; Lobet et al., 2013).

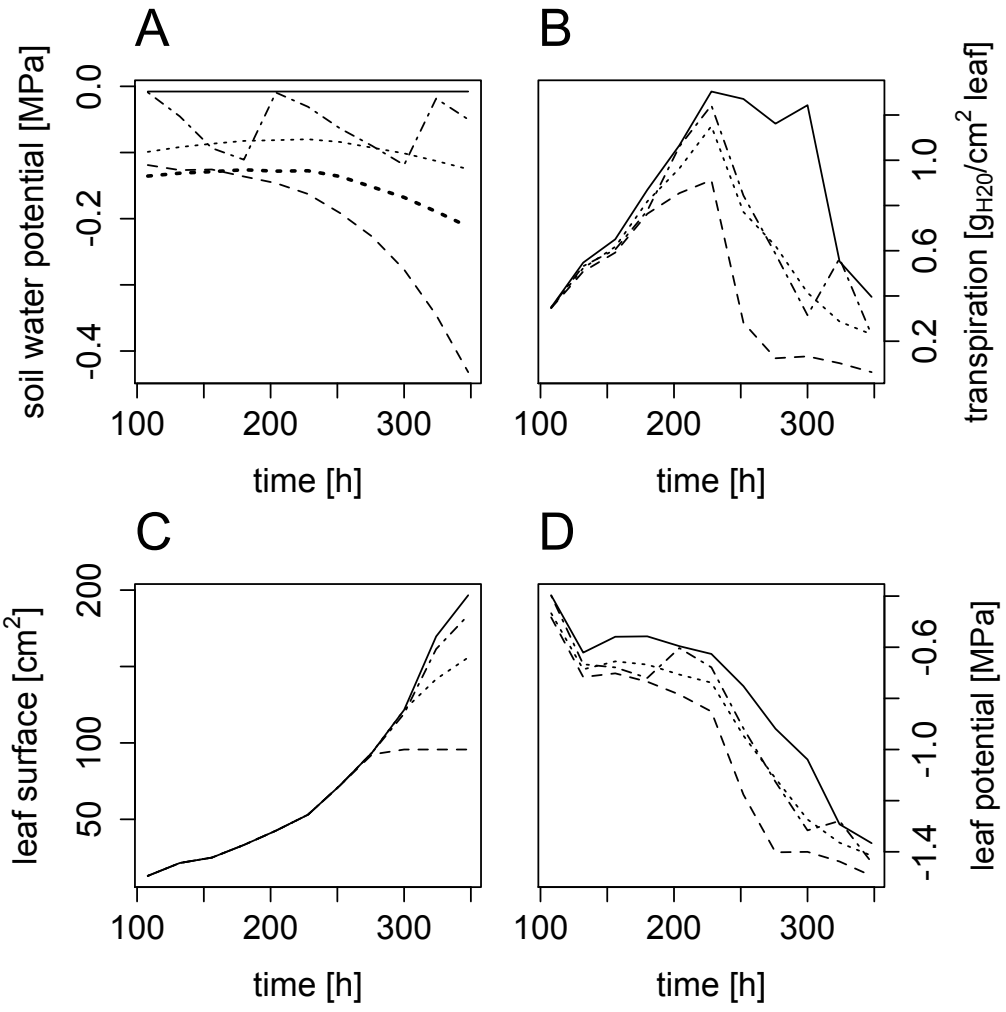

Figure 7: Effect of the irrigation technique on the plant water status. A. Average soil water content at the vicinity of the roots. B. Transpiration rate. C. Total leaf surface. D. Leaf water potential. Plain lines: WW. Dashed lines: WS. Dotted lines: PRD (all). Bold dotted line: PRD (dry compartment). Dashed-dotted lines: RW. Values were taken at 12:00 at every day of the simulation.

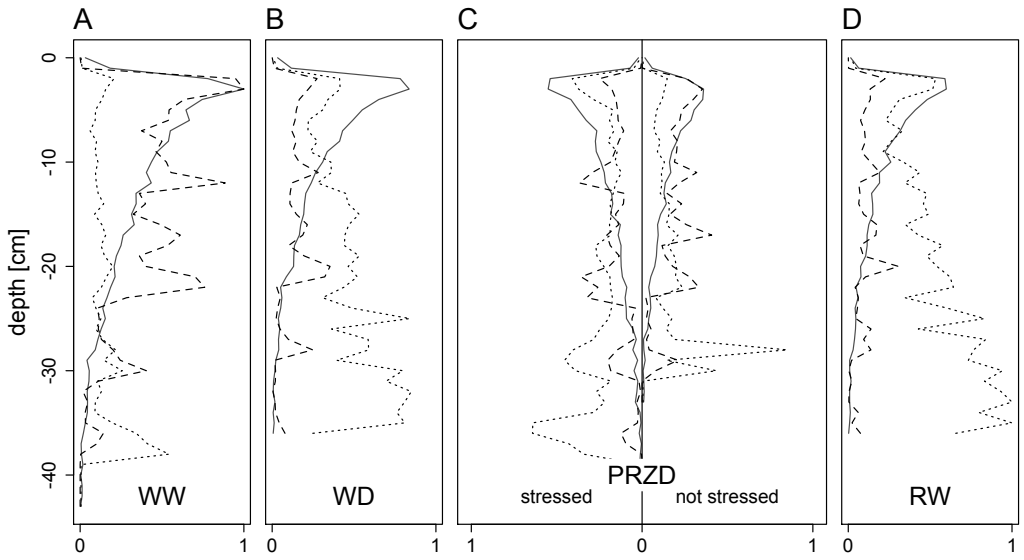

Figure 8: Effect of the irrigation technique on the roots: A. well watered, B. water deficit, C. partial root zone drying (left panel: water stress; right panel: well watered) and D. re-watering. Plain grey lines represent the root surface (sum per depth), dashed lines represent the water uptake (sum per depth) and dotted lines represent the root water potential (unsigned average per depth). All values are normalized to the maximal value of each variable across all scenarios.

PlaNet-Maize effectively reproduces the effect of different irrigation practices that are generally observed experimentally. As a general rule, decreasing the amount of available water for the plant reduces its transpiration and, above a certain threshold, decreases plant growth as well (fig. 7.

However, PlaNet-Maize could not capture experimental difference classically observed between PRD and RW treatment. Indeed, a growing body of evidence indicates that PRD has a beneficial influence on the plant water consumption and yield compared to RW (as an example, see the works of Dodd (2007) and Kang et al. (2000)). In these experiments, no major differences in leaf water potential were observed (as in our simulations, fig. 7.C), but significant differences in final yield were recorded between the treatments. Evidently, the transpiration assimilation feedback that is used in PlaNet-Maize is not able to simulate this response. For this to work, the instantaneous WUE coefficient should be adjusted as a function of the soil water potential sensed by the plant.

The yield response to PRD is generally explained by differences in abscissic acid (ABA) production in the roots. It seems plausible from our simulations that a root signal informing leaves about the soil water potential might be sufficient to adjust stomatal conductance and restore a leaf water potential equivalent to the WW. This would reduce assimilation on the short term but would save water for future use. Including ABA signalling in PlaNet-Maize might thus help to reproduce the typical yield response to PRD treatment. This would lead ultimately to an apparent adjustment

of the instantaneous WUE coefficient as a function of the soil water potential.

Based on the response of the leaf water potential (ψ_{leaf}) to decrease in soil water potential (ψ_{soil}), plant can exhibit either an isohydric (ψ_{leaf} remains constant under decreasing ψ_{soil}) or anisohydric (ψ_{leaf} decreases under decreasing ψ_{soil}) behaviour. In our model, ψ_{leaf} tends to decrease with a decreasing ψ_{soil}, which suggest an anisohydric behaviour (fig. 9). However, experimental data have shown the opposite in the fields, hence labelling maize as an isohydric plant (Tardieu et al., 1992; Ben Haj Salah and Tardieu, 1997). Such isohydric behaviour has been characterised by an interplay between g_s, ψ_{leaf} and the concentration of ABA in the xylem sap (Tardieu and Simonneau, 1998). Implementing ABA in PlaNet-Maize should help enabling an isohydric behaviour in our simulations.

4.4. Regulation sensibility

The results of the analysis on g_s are given in figures 10.1A-1C and 11.1A-1C. Increasing the sensibility of g_s to the water potential leads to early stomatal closure which causes the reduction of transpiration and the maintenance of a high water potential. This does not affect root conductances but has a dramatic impact on plant growth and leaf area. Fortunately, the saved water is available later and allows plants to transpire for a longer period (fig. 10.1C, arrow). On the opposite, decreasing the sensibility of g_s to the water potential leads to stomata being more open, a higher transpiration and a rapid decrease of the plant water potential, which causes and expected decrease of the root radial conductance and increase of xylem cavitation.

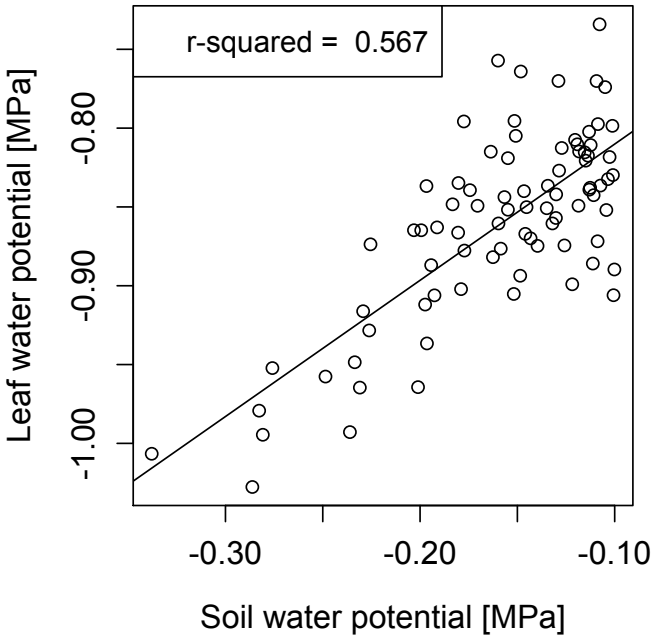

Figure 9: Response of leaf water potential to soil drying in PlaNet-Maize.

The changes in the sensibility of K_r (figs. 10.2A-2C and 11.2A-2C) and K_x (figs. 10.3A-3C and 11.3A-3C) have smaller effect on the plant water status compared to g_s. The largest effects are seen under faster K_r response, where a rapid reduction of the root radial conductivity leads to a sensible reduction of the plant water potential, stomatal opening and transpiration. Interestingly, this effect was obtained without any consequences on growth and leaf area and appears thus as plausible way to achieve conservative water use. Neither delayed K_r nor altered K_x responses have important consequences on the plant water dynamics.

Contrasting transpiration dynamics were thus observed between plants with modified g_s and K_r responses. On the one side, the delayed g_s response causes the plant to follow the evaporative demand at the cost of a quick drying of the soil, and is therefore valuable in conditions where water supply is non limiting. On the other side, the faster g_s and K_r responses lead to a conservative use of water that allows transpiration maintenance later in the season. Recent experimental data suggest that such water saving strategy during the vegetative growth is correlated with terminal drought resistance (Zaman-Allah et al., 2011a,b; Kholová et al., 2010; Tardieu, 2011). Some of our simulations differed from these results by the strong reduction in plant size which was not observed in field conditions. It has to be noted, however, that the drought susceptible and resistant genotypes used in these experiments did not differ necessarily by those mechanisms that are considered in our simulations.

Beyond their effect on the plant water dynamics, the modifier functions also change the spatial patterns of water extraction by roots in slightly different ways. These modifications rely mostly on the changes of radial vs axial root conductivities, as a large K_r/K_x ratio tends to concentrate water uptake in the upper layers, while a lower ratio tends to distribute the uptake vertically (Draye et al., 2010). This is most noticeable in the K_r sensitivity analysis where the K_r/K_x ratio increases under a delayed response of K_r and decreases under a faster response (fig. 11). As a consequence, the uptake pattern is decreased by a constant value under the faster K_r response while it is increased in upper layers under the delayed K_r response.

These sensitivity analyses emphasize the interplay between the regulation of g_s, K_r and K_x. Obviously, making these regulations all dependent on the local water potential is largely responsible for this interplay, but this only reflects the structural integration of these regulations which all contribute to the same water flow. It follows that the classical experimental methodology consisting in the manipulation of a single regulating mechanism should be complemented with at least some characterisation of how this manipulation could affect the other mechanisms. PlaNet-Maize provides the required framework to integrate many different factors influencing the water dynamics.

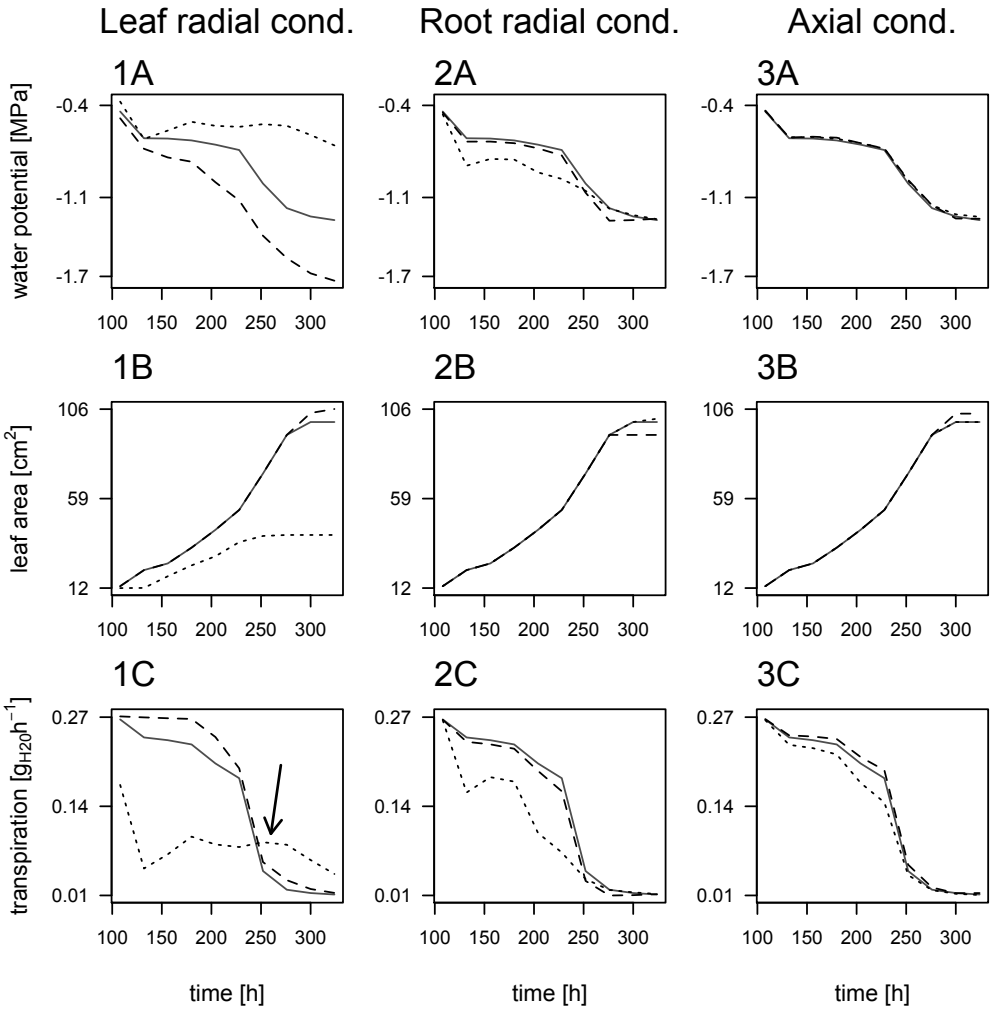

Figure 10: Effect of the regulation processes on the plant water status. 1-. changed regulation of leaf radial conductivity; 2-. changed regulation of root radial conductivity; 3-. changed regulation of axial conductance; -A. evolution of the collar water potential; -B. evolution of shoot surface; -C. evolution of the relative transpiration (to the leaf area). Plain lines represent the controls, with no modification of the regulation processes, dashed lines represents the inhibited regulation processes and dotted lines represent the enhanced regulation processes.

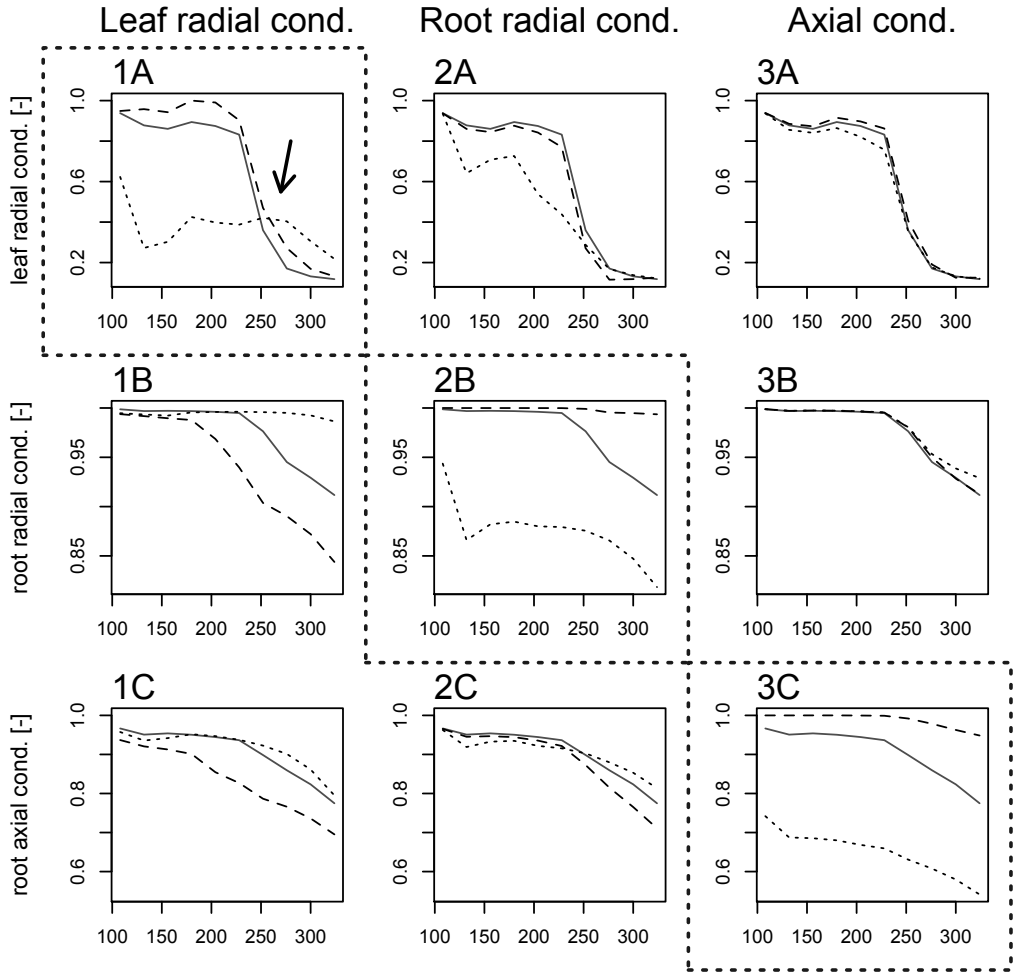

Figure 11: Effect of the regulation processes on the plant water status. 1-. changed regulation of leaf radial conductivity; 2-. changed regulation of root radial conductivity; 3-. changed regulation of axial conductance; -A. evolution of the leaf radial conductivity; -B. evolution of the root radial conductivity; -C. evolution of the root axial conductance. Plain lines represent the controls, with no modification of the regulation processes, dashed lines represents the inhibited regulation processes and dotted lines represent the enhanced regulation processes. Framed plots highlight the differences in regulation sensibility for each scenario.

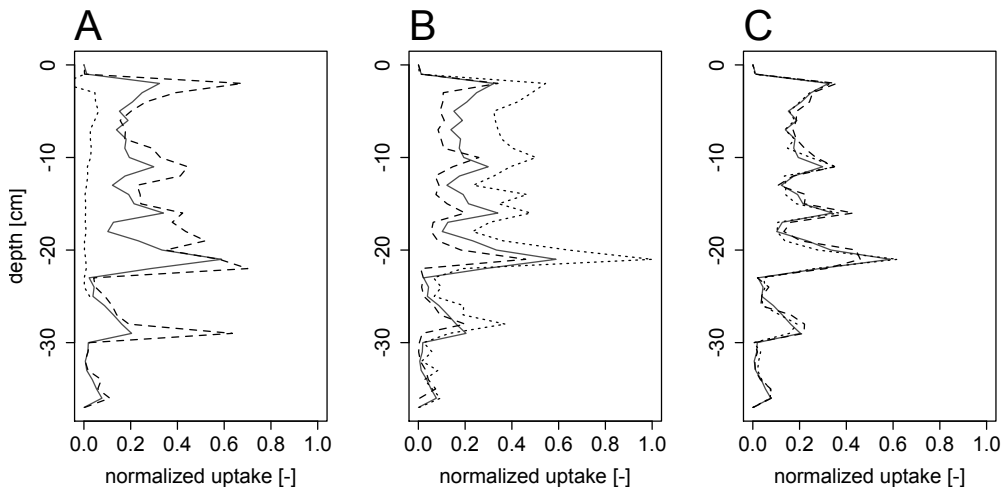

Figure 12: Effect of the regulation processes on the root water uptake profiles. A. modified leaf radial conductivity; B. modified root radial conductivity; C. modified axial conductance. Plain grey lines represent the controls, with no modification of the regulation processes, dashed lines represents the inhibited regulation processes and dotted lines represent the enhanced regulation processes. All values are normalized.

5. Conclusions and perspectives

5.1. Functional-structural modeling as a useful tool to decrypt plant water relations

It is now commonly accepted that functional-structural models are essential tools to access the complexity of plant systems (Tardieu, 2010; Godin and Sinoquet, 2005). They allow scientists to investigate the dynamics of complex systems and unravel the effect of multiple regulation mechanisms (Hill et al., 2013).

PlaNet-Maize was successfully used to simulate water flows in the entire plant continuum with a resolution down to the plant element level. This first version of the model was able to reproduce the effect of root architecture and hydraulic properties on the water relations in the plant as previously shown in former models (Draye et al., 2010; Janott et al., 2011). In addition, by implementing simple regulatory processes acting on the local values of K_r and K_x, we found that the virtual plant was able to tightly control its water status.

Divergences were observed between experimental and modeling results for contrasted water management practices. PlaNet-Maize was not able to reproduce the beneficial effect of PRD over RW treatment. This difference appeared supposably because a finer signaling of local soil conditions (via the production and translocation of ABA) was not implemented in the model.

Finally, PlaNet-Maize was used to show the effect of modified sensibilities

for the different regulation sites. Enhanced sensibilities enable the plant to react more quickly to environmental constrain and therefore to have conservative water use behaviors. Results show that changing the sensibilities at the root system level (either K_x and/or K_r) can have a non-negligible effect on the plant water status by increasing its overall water use efficiency.

5.2. Envisaged model development

A first envisaged development path for PlaNet-Maize would be the improvement of its water-related modules. Firstly, in order to model more realistic condition and test the influence of different soil environment, integration of a more realistic soil module, such as Hydrus or R-SWMS (Javaux et al., 2008), is required. Moreover, as discussed previously, the implementation of a long distance signal between the root and the shoot, such as ABA, should be implemented to enable a finer sensing of the local variations in the soil water content.

A second direction for the development of the model would be to link it with lower scale models, down to the cell level (Band et al., 2012). Indeed, the modular nature of the PlaNet based models allows an easy and straightforward integration with other models.

Finally, a third direction would be to extend the model from vegetative to reproductive stages, in order to assess the effect of terminal drought stress on grain formation and, ultimately, yield. Again, the modular structure of PlaNet-Maize easily allows the creation of new article types needed to simulate flowering and grain filling.

5.3. Future experimental needs

Functional-structural plant models rely on quantitative data to be accurate and representative of the reality. Unfortunately, in some area, notably regarding plant hydraulics, this quantitative knowledge is missing. As functional-structural models are now recognized as useful tools for the plant science community (Tardieu, 2010; Hill et al., 2013), more and more modeling projects arise and therefore there is an increasing need for more quantitative biological data. In particular, more data are needed to characterise hydraulic properties of the different plant organs as function of endogenous (e.g. age, type and order of root segments) and exogenous factors (e.g. response curves to drying soil).

6. Acknowledgments

This research was funded by a grant from the Fond pour la formation à la Recherche dans l'Industrie et dans l'Agriculture to GL, the grant IAP7/29 from the Belgian Science Policy Office and the grant ARC-1116-036 from the Communauté française de Belgique to XD.

The authors would like to thanks Vincent Larondelle for its useful help in the model development.

References

Allen, Jr., L.H., Kakani, V.G., Vu, J.C.V., Boote, K.J., 2011. Elevated CO2 increases water use efficiency by sustaining photosynthesis of water-limited maize and sorghum. Journal of Plant Physiology 168, 1909–1918.

584 Band, L.R., Fozard, J.A., Godin, C., Jensen, O.E., Pridmore, T., Bennett,
585 M.J., King, J.R., 2012. Multiscale Systems Analysis of Root Growth and
586 Development: Modeling Beyond the Network and Cellular Scales. The
587 Plant Cell 24, 3892–3906.

588 Ben Haj Salah, H., Tardieu, F., 1997. Control of Leaf Expansion Rate of
589 Droughted Maize Plants under Fluctuating Evaporative Demand. Plant
590 Physiology , 893–900.

591 Bidel, L., Pagès, L., Riviere, L., Pelloux, G., Lorendeau, J., 2000. Mass-
592 FlowDyn I: A Carbon Transport and Partitioning Model for Root System
593 Architecture. Annals of Botany 85, 869–886.

594 Bohrer, G., Mourad, H., Laursen, T.A., Drewry, D., Avissar, R., Poggi,
595 D., R, O., Katul, G.G., 2005. Finite element tree crown hydrodynamics
596 model (FETCH) using porous media flow within branching elements: a
597 new representation of tree hydrodynamics. Water Resources Research 41,
598 1–17.

599 Bramley, H., Turner, N., Turner, D., Tyerman, S.D., 2009. Roles of Mor-
600 phology, Anatomy, and Aquaporins in Determining Contrasting Hydraulic
601 Behavior of Roots. Plant Physiology 150, 348–364.

602 Cochard, H., 2002. Xylem embolism and drought-induced stomatal closure
603 in maize. Planta 215, 466–471.

604 Couvreur, V., Vandenborg, J., Javaux, M., 2012. A simple three-dimensional
605 macroscopic root water uptake. Hydrology and Earth System Sciences 16,
606 2957–2971.

607 Damour, G., Simonneau, T., Cochard, H., Urban, L., 2010. An overview of
608 models of stomatal conductance at the leaf level. Plant, Cell and Environ-
609 ment 33, 1419–1438.

610 Diggle, A.J., 1988. ROOTMAP—a model in three-dimensional coordinates
611 of the growth and structure of fibrous root systems. Plant and Soil 105,
612 169–178.

613 Dodd, I.C., 2007. Soil moisture heterogeneity during deficit irrigation alters
614 root-to-shoot signalling of abscisic acid. Functional Plant Biology 34, 439–
615 448.

616 Doussan, C., Pierret, A., Garrigues, E., Pagès, L., 2006. Water Uptake by
617 Plant Roots: II – Modelling of Water Transfer in the Soil Root-system
618 with Explicit Account of Flow within the Root System – Comparison with
619 Experiments. Plant and Soil 283, 99–117.

620 Doussan, C., Vercambre, G., Pagès, L., 1998. Modelling of the hydraulic
621 architecture of root systems: and integrated approach to water absorption
622 - Distribution of axial and radial conductances in maize. Annals of Botany
623 81, 225–232.

624 Draye, X., Kim, Y., Lobet, G., Javaux, M., 2010. Model-assisted integration
625 of physiological and environmental constraints affecting the dynamic and
626 spatial patterns of root water uptake from soils. Journal of Experimental
627 Botany 61, 2145–2155.

628 Draye, X., Pagès, L., 2006. CrossTalk: a simulation platform for the linking

of existing soil, plant and atmosphere models. IEEE-Conference Proceding Service PM06, 95–100.

Drouet, J.L., Pagès, L., 2003. GRAAL: a model of GRowth, Architecture and carbon ALlocation during the vegetative phase of the whole maize plant. Model description and parametrisation. Ecological Modelling 165, 143–173.

Drouet, J.L., Pagès, L., 2007. GRAAL-CN: A model of GRowth, Architecture and ALlocation for Carbon and Nitrogen dynamics within whole plants formalised at the organ level. Ecological Modelling 206, 231–249.

Enstone, D.E., Peterson, C.A., Ma, F., 2003. Root Endodermis and Exodermis: Structure, Function, and Responses to the Environment. Journal of Plant Growth Regulation 21, 335–351.

Fournier, C., Andrieu, B., 1998. A 3D Architectural and Process-based Model of Maize Development. Annals of Botany 81, 233–250.

Ge, Z., Rubio, G., Lynch, J.P., 2000. The importance of root gravitropism for inter-root competition and phosphorus acquisition efficiency: results from a geometric simulation model. Plant and Soil 218, 159–171.

van Genuchten, M., 1980. A closed-form equation for predicting the hydraulic conductivity of unsaturated soils. Soil Science Society of America Journal 44, 891–898.

Girardin, P., 2000. Ecophysiologie du maïs. Association Generale des Producteurs de Maïs, Montardon.

651 Godin, C., Sinoquet, H., 2005. Functional-structural plant modelling. New
652 Phytologist 166, 705–708.

653 Hacke, U.G., Sperry, J.S., Ewers, B.E., Ellsworth, D.S., Schäfer, K.V.R., RR,
654 O., 2000a. Influence of soil porosity on water use in Pinus taeda. Oecologia
655 124, 495–505.

656 Hacke, U.G., Sperry, J.S., Pittermann, J.J., 2000b. Drought experience and
657 cavitation resistance in six shrubs from the Great Basin, Utah. Basic and
658 Applied Ecology 1.

659 Hill, K., Porco, S., Lobet, G., Zappala, S., Mooney, S., Draye, X., Ben-
660 nett, M.J., 2013. Root Systems Biology: bridging regulatory networks to
661 rhizosphere-scale processes. Plant Physiology .

662 Hochholdinder, F., Park, W.J., Sauer, M., Woll, K., 2004. From weeds to
663 crops: genetic analysis of root development in cereals. TRENDS in Plant
664 Science 9, 42–48.

665 Holbrook, N.M., Zwieniecki, M., 1999. Embolism Repair and Xylem Tension:
666 Do We Need a Miracle? Plant Physiology 120, 7–10.

667 Hu, T., Kang, S., Li, F., Zhang, J., 2011. Effects of partial root-zone irri-
668 gation on hydraulic conductivity in the soil-root system of maize plants.
669 Journal of Experimental Botany 62, 4163–4172.

670 Janott, M., Gayler, S., Gessler, A., Javaux, M., Klier, C., Priesack, E., 2011.
671 A one-dimensional model of water flow in soil-plant systems based on plant
672 architecture. Plant and Soil 341, 233–256.

673 Jarvis, P.G., 1976. The Interpretation of the Variations in Leaf Water Poten-
674 tial and Stomatal Conductance Found in Canopies in the Field. Philosoph-
675 ical Transactions of the Royal Society B: Biological Sciences 273, 593–610.

676 Javaux, M., Schroeder, T., Vanderborght, J., Vereecken, H., 2008. Use of
677 a three-dimensional detailed modeling approach for predicting root water
678 uptake. . Vadose Zone Journal 7, 1079–1088.

679 Javot, H., Maurel, C., 2002. The role of aquaporins in root water uptake.
680 Annals of Botany 90, 301–313.

681 Kang, S., Liang, Z., Pan, Y., Shi, P., 2000. Alternate furrow irrigation for
682 maize production in an arid area. Agricultural water management 45,
683 267–274.

684 Kholová, J., Hash, C.T., Kakkera, A., Kocová, M., Vadez, V., 2010. Con-
685 stitutive water-conserving mechanisms are correlated with the terminal
686 drought tolerance of pearl millet [Pennisetum glaucum (L.) R. Br.]. Jour-
687 nal of Experimental Botany 61, 369–377.

688 Landsberg, J., Fowkes, N., 1978. Water movement through plant roots.
689 Annals of Botany 42, 493–508.

690 Li, Y., Sperry, J.S., Shao, M., 2009. Hydraulic conductance and vulnerability
691 to cavitation in corn (Zea mays L.) hybrids of differing drought resistance.
692 Environmental and Experimental Botany 66, 341–346.

693 Lobet, G., Hachez, C., Chaumont, F., Javaux, M., Draye, X., 2013. Root wa-
694 ter uptake and water flow in the soil-root domain, in: Eshel, A., Beeckman,
695 T. (Eds.), Plant Roots: The Hidden Half. CRC Press, New york.

Lynch, J.P., Nielsen, K.L., Davis, R.D., Jablokow, A.G., 1997. SimRoot: Modelling and visualization of root systems. Plant and Soil 188, 139–151.

Maurel, C., Verdoucq, L., Luu, D., Santoni, V., 2008. Plant aquaporins: membrane channels with multiple integrated functions. Annual Review of Plant Biology 59, 595–624.

McCully, M.E., Huang, C.X., Ling, L.E.C., 1998. Daily embolism and refilling of xylem vessels in the roots of field-grown maize. New Phytologist 138, 327–342.

Mollier, A., PEllerin, S., 1999. Maize root system growth and development as influenced by phosphorus deficiency. Journal of Experimental Botany 50, 487–497.

Pagès, L., Jordan, M.O., Picard, D., 1989. A simulation model of the three-dimensional architecture of the maize root system. Plant and Soil 119, 147–154.

Pagès, L., Vercambre, G., Drouet, J.L., Lecompte, F., Collet, C., LeBot, J., 2004. RootTyp: a generic model to depict and analyse the root system architecture. Plant and Soil 258, 103–119.

Peirce, G.J., 1936. The State of Water in Ducts and Tracheids. Plant Physiology 11, 623–628.

Postma, J.A., Lynch, J.P., 2011. Theoretical evidence for the functional benefit of root cortical aerenchyma in soils with low phosphorus availability. Annals of Botany 107, 829–841.

718 Somma, F., Hopmans, J., Clausnitzer, V., 1998. Transient three-dimensional
719 modeling os soil water and solute transport with simultaneous growth, root
720 water and nutrient uptake. Plant and Soil 202, 281–293.

721 Sperry, J.S., Adler, F.R., Campbell, G.S., Comstock, J.P., 1998. Limitation
722 of plant water use by rhizosphere and xylem conductance: results from a
723 model. Plant, Cell and Environment 21, 347–359.

724 Sperry, J.S., Donnelly, J.R., Tyree, M.T., 1988. Seasonal Occurrence of
725 Xylem Embolism in Sugar Maple (Acer saccharum). American Journal of
726 Botany 75, 1212–1218.

727 Steudle, E., 2001. The cohesion-tension mechanism and the acquisition of
728 water by plant roots. Annual Review of Plant Physiology and Plant Molec-
729 ular Biology 53, 847–875.

730 Steudle, E., Peterson, C.A., 1998. How does water get through roots? Journal
731 of Experimental Botany 49, 775–788.

732 Tardieu, F., 2010. Why work and discuss the basic principles of plant mod-
733 elling 50 years after the first plant models? Journal of Experimental
734 Botany 61, 2039–2041.

735 Tardieu, F., 2011. Any trait or trait-related allele can confer drought tol-
736 erance: just design the right drought scenario. Journal of Experimental
737 Botany 63, 25–31.

738 Tardieu, F., Simonneau, T., 1998. Variability among species of stomatal con-
739 trol under fluctuating soil water status and evaporative demand: modelling

isohydric and anisohydric behaviours. Journal of Experimental Botany 49, 419–432.

Tardieu, F., Zhang, J., Katerji, N., Bethenod, O., Palmer, S., Davies, W.J., 1992. Xylem ABA controls the stomatal conductance of field-grown maize subjected to soil compaction or soil drying. Plant, Cell and Environment 15, 193–197.

Tyree, M.T., Sperry, J.S., 1989. Vulnerability of Xylem to Cavitation and Embolism. Annual Review of Plant Physiology and Plant Molecular Biology 40, 19–36.

Wei, C., Tyree, M.T., Steudle, E., 1999. Direct Measurement of Xylem Pressure in Leaves of Intact Maize Plants. A Test of the Cohesion-Tension Theory Taking Hydraulic Architecture into Consideration. Plant Physiology 121, 1191–1205.

Zaman-Allah, M., Jenkinson, D.M., Vadez, V., 2011a. A conservative pattern of water use, rather than deep or profuse rooting, is critical for the terminal drought tolerance of chickpea. Journal of Experimental Botany 62, 4239–4252.

Zaman-Allah, M., Jenkinson, D.M., Vadez, V., 2011b. Chickpea genotypes contrasting for seed yield under terminal drought stress in the field differ for traits related to the control of water use. Functional Plant Biology 38, 270.

Zwieniecki, M.A., Holbrook, N.M., 2009. Confronting Maxwell's demon:

762 biophysics of xylem embolism repair. TRENDS in Plant Science 14, 530–
763 534.